Organometallics 1992, *11*, 1937-1948

New Neutral and Ionic Methyl and Chloro Palladium and Platinum Complexes Containing Hemilabile Phosphorus-Nitrogen Ligands. Study of the Insertion of Carbon Monoxide into the Metal-Methyl Bond

Guido P. C. M. Dekker, Albert Buijs, Cornelis J. Elsevier, and Kees Vrieze*

Anorganisch Chemisch Laboratorium, J. H. van 't Hoff Instituut, University of Amsterdam,
Nieuwe Achtergracht 166, 1018 WV Amsterdam, The Netherlands

Piet W. N. M. van Leeuwen

Department of Chemical Engineering, J. H. van 't Hoff Instituut, University of Amsterdam,
Nieuwe Achtergracht 166, 1018 WV Amsterdam, The Netherlands

Wilberth J. J. Smeets and Anthony L. Spek

Bijvoet Center for Biomolecular Research, vakgroep Kristal- en Structuurchemie,
University of Utrecht, Padualaan 8, 3584 CH Utrecht, The Netherlands

Yuan F. Wang and Casper H. Stam

Laboratorium voor Kristallografie, J. H. van 't Hoff Instituut, University of Amsterdam,
Nieuwe Achtergracht 166, 1018 WV Amsterdam, The Netherlands

Received October 21, 1991

The synthesis and properties are described for the complexes (PAN)MCl_2 (M = Pd(II), Pt(II)), $(PAN)_2PdCl_2$, $[(PAN)M(CH_3)]^+Y^-$ (M = Pd(II); Y^- = Cl^-, $SO_3CF_3^-$, BF_4^-), and $[(PAN)M(CH_3)(CH_3CN)]^+Y^-$ (M = Pd(II), Pt(II); Y^- = $SO_3CF_3^-$, BF_4^-) and further $(PC_3N)M(CH_3)Cl$ (M = Pd(II), Pt(II)) and $[(PC_3N)Pd(CH_3)(CH_3CN)]^+SO_3CF_3^-$, where PAN is the rigid ligand 1-(dimethylamino)-8-(diphenylphosphino)naphthalene and PC_3N the more flexible ligand 1-(dimethylamino)-3-(diphenylphosphino)propane. For $(PAN)_2PdCl_2$, in which PAN acts as a monodentate phosphorus-bonded ligand, and for $(PAN)Pd(CH_3)Cl$, in which PAN is a chelate, single-crystal X-ray structure determinations were carried out: $(PAN)_2PdCl_2$, space group $P\bar{1}$, a = 12.837 (2) Å, b = 17.518 (3) Å, c = 10.788 (3) Å, α = 91.07 (2)°, β = 112.87 (2)°, γ = 100.27 (2)°, V = 2189.1 (6) Å^3, Z = 2, R = 0.044, R_w = 0.065; $(PAN)Pd(CH_3)Cl$, space group $P2_1/n$, a = 11.418 (1) Å, b = 15.088 (1) Å, c = 12.434 (1) Å, β = 99.81 (1)°, V = 2110.7 (3) Å^3, Z = 4, R = 0.025, R_w = 0.026. The investigations were mainly focused on the study of the carbonylation of the metal-carbon bond and in particular on the influence of the type of metal and ligand on the intimate steps of the mechanisms of the metal-acyl bond formation and on the magnitude of the rates. In the case of the reaction of $(P\text{-}N)Pt(CH_3)Cl$ (CH_3 cis to P) evidence has been obtained for the formation of three intermediates with a terminal CO group in which the P-N (P-N = PAN, PC_3N) ligand temporarily functions as a monodentate phosphorus-bonded ligand, i.e. [trans P, cis CH_3 (Pt-CO)], [cis P, trans CH_3 (Pt-CO)], and [cis P, cis CH_3 (Pt-CO)], which for the first time were observed to occur together in one system. Subsequently the formation of the final metal-acyl product $(P\text{-}N)Pt(C(O)CH_3)Cl$ ($C(O)CH_3$ cis to P) could be observed, in which the P-N ligand is again chelate-bonded. However, during the carbonylation of $[(PAN)Pd(CH_3)]^+Y^-$ and $[(PAN)Pd(CH_3)(CH_3CN)]^+Y^-$ (Y^- = $SO_3CF_3^-$, BF_4^-), only the intermediate $[(PAN)Pd(CH_3)(CO)]^+Y^-$ (CH_3 cis to P) could be detected, with the P-N ligand in the chelating form, before the formation of the acyl products $[(PAN)Pd(C(O)CH_3)]^+Y^-$ and $[(PAN)Pd(C(O)CH_3)(CH_3CN)]^+Y^-$, in which the $C(O)CH_3$ group is cis to P. Several isomerization reactions are necessary to obtain these products. The reaction rates, in terms of half-life times $t_{1/2}$, were measured at 25 bar of CO in CD_2Cl_2 by means of NMR spectroscopy in a high-pressure tube and were compared with data for analogous bpy, dppp, and dppe complexes. The results show that generally the complexes with good leaving groups Y^- in noncoordinating solvents reacted much faster than the chloride complexes. The influence of the metal and the bidentate ligands on the insertion is reflected in a decrease in rates in the order Pd(II) > Pt(II) and bpy > PAN > PC_3N > dppp > dppe for $(L\text{-}L)Pt(CH_3)Cl$ and bpy > dppp ≫ PAN > PC_3N > dppe for $(L\text{-}L)Pd(CH_3)Cl$, while for $[(L\text{-}L)Pd(CH_3)(CH_3CN)]^+SO_3CF_3^-$ the rate decreased in the order bpy > dppp > PC_3N > PAN > dppe. Some general considerations are presented to rationalize the trends in the rates.

Introduction

Carbonylation reactions are of fundamental interest and constitute a key step in, for example, hydroformylation, alkoxycarbonylation, and polyketone production.[1] For Pd- and Pt-catalyzed carbonylation, mechanistic studies have mainly focused on the carbonylation of aryl complexes containing monodentate phosphines.[2] For example, it was shown by Garrou and Heck that migration of an aryl group to CO may proceed via a slow reaction involving a five-coordinate intermediate or via a four-coordinate complex after dissociation of one phosphine ligand.[3] This reaction was studied in more detail by Anderson et al.[2] (and ref-

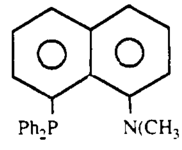

PAN (1)

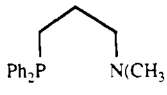

PC_3N (8)

Figure 1. 1-(Dimethylamino)-8-(diphenylphosphino)naphthalene (PAN; 1) and 1-(dimethylamino)-3-(diphenylphosphino)propane (PC_3N; 8).

---

* To whom correspondence should be addressed.

0276-7333/92/2311-1937$03.00/0

Table I. Numbering of the Complexes Studied

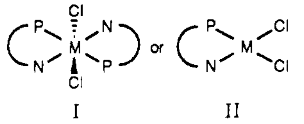

P–N = PAN (1)

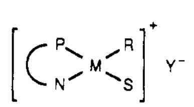

M		S	Y^-	P–N = PAN (1)		P–N = PC_3N (8)	
				R = CH_3	R = C(O)CH_3	R = CH_3	R = C(O)CH_3
Pt	2 (II)		Cl^-	**4a**	**6a**	9	11
			$SO_3CF_3^-$	**4b**	**6b**		
			BF_4^-	**4c**	**6c**		
		CH_3CN	$SO_3CF_3^-$	**4d**	**6d**		
		CH_3CN	BF_4^-	**4e**	**6e**		
Pd	**3a** (II)		Cl^-	**5a**	**7a**	**10a**	**12a**
	3b (I)		$SO_3CF_3^-$	**5b**	**7b**	**10b**	**12b**
			BF_4^-	**5c**	**7c**		
		CH_3CN	$SO_3CF_3^-$	**5d**	**7d**		
		CH_3CN	BF_4	**5e**	**7e**		

Scheme I. Sequence Proposed for the Carbonylation of the Pt–R bond in L_2PtRX ($R = Ph$, $X^- = Cl^-$, $L = PPh_3$)[a]

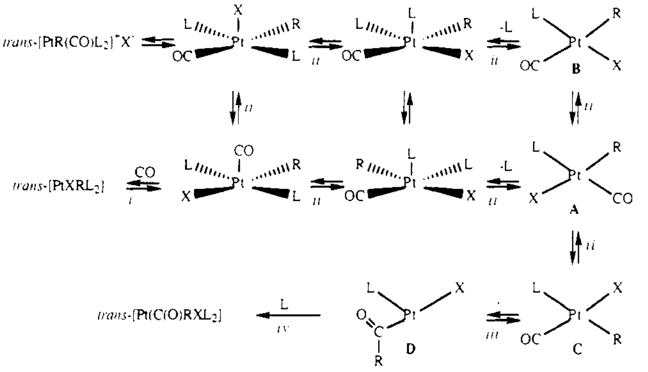

[a] Legend: (i) addition of the CO molecule to the Pt center; (ii) pseudorotations and isomerization of various Pt–CO intermediates (A–C); (iii) migration of the R group to the cis-coordinated CO molecule; (iv) stabilization of the unsaturated product (D) by ligand association.[2]

erences cited therein). Association of CO to the Pt center (i), pseudorotations and isomerization of the four- and five-coordinate Pt–CO intermediates (ii), and dissociation of one phosphine ligand, L, may produce three square-planar intermediates (Scheme I): [trans L, cis R (Pt–CO)] (A), [cis L, trans R (Pt–CO)] (B), and eventually [cis L, cis R (Pt–CO)] (C).

Not taken into account was the possibility of dissociation of the chloride anion. It was proposed that via intermediate C the unsaturated aroyl intermediate D (iii) and finally the aroyl product *trans*-[$L_2Pt(C(O)Ph)Cl$] via recoordination of the PPh_3 ligand (iv) are formed (Scheme I). For none of the examples investigated could the whole process be studied in detail in one reaction sequence. In the case of L = PPh_3 only intermediates A and B were observed and not C. It has been demonstrated that C, prepared in a separate experiment,[4] indeed led to the final aroyl product. In the same publication[4] it was reported that complexes (L-L')Pt(Ph)Cl (L-L' = 1,2-bis(diphenylphosphino)ethane (dppe), 1-(diphenylarsino)-2-(diphenylphosphino)ethane (appe)) appeared to be unreactive in the carbonylation of the Pt–aryl bond. However, in 1985 Anderson and Lumetta[5] extended this study and reported a series of slow CO insertion reactions for compounds (L-L')Pt(Ph)Cl (L-L' = dppe, appe, 1-(dimethylamino)-2-(diphenylphosphino)ethane (PC_2N), 1-(diphenylphosphino)-2-(methylthio)ethane (PC_2S), 1,3-bis(diphenylphosphino)propane (dppp)), for which the insertion rate decreased in the order dppp > PC_2S > PC_2N ≫ appe, dppe. Although little evidence was given for the mechanism, it was proposed that dppp, dppe, and appe remained bonded in a bidentate fashion during the carbonylation reaction, while it was suggested that the hemilabile PC_2N and PC_2S ligands reacted via dissociation of the N and S donor atoms, respectively. The aforementioned studies were all carried out for metal–aryl complexes, while relatively little work has been reported on bidentate palladium- and platinum–methyl complexes.[6-9]

Regarding the actual migratory-insertion step, attention has been paid to theoretical investigations.[10] In addition, recently in the case of Mo complexes fast equilibria have been observed, not only between methyl–carbonyl complexes and the isomeric bidentate η^2-acyl species, which already was quite well-known,[11] but also with agostic acyl species perhaps being involved in fast equilibria together with the former two species.[12]

---

(1) Wender, I., Pino, P., Eds. *Organic Synthesis via Metal Carbonyls*; Wiley: New York, 1977; Vol. 2. Falbe, J., Ed. *New Synthesis with Carbon Monoxide*; Springer-Verlag: New York, 1980. Collman, J. P.; Hegedus, L. S.; Norton, J. R.; Finke, R. G. *Principles and Applications of Organotransition Metal Chemistry*; University Science Books: Mill Valley, CA, 1987; pp 356–376. Parshall, G. W. *Homogeneous Catalysis*; Wiley: New York, 1980. Calderazzo, F. *Angew. Chem.* **1977**, *89*, 305. Kuhlmann, E. J.; Alexander, J. J. *Coord. Chem. Rev.* **1980**, *33*, 195. Cardaci, G.; Reichenbach, G.; Bellachioma, G.; Wassink, B.; Baird, M. C. *Organometallics* **1988**, *7*, 2475. Gouch, A. Brit. Patent 081304, 1967. Fenton, D. M. U.S. Patent 3530109, 1970. Nozaki, K. U.S. Patent 3694412, 1972, and other patents by the same group. Shryne, T. M.; Voller, H. V. U.S. Patent 3984388, 1976. Drent, E. Eur. Pat. Appl. 121965, 1984, and other patents by the same group. Sen, A. CHEMTECH **1986**, 48.

(2) Anderson, G. K.; Cross, R. J. *Acc. Chem. Res.* **1984**, *17*, 67.

(3) Garrou, P. E.; Heck, R. F. *J. Am. Chem. Soc.* **1976**, *98*, 4115.

(4) Anderson, G. K.; Clark, H. C.; Davies, J. A. *Inorg. Chem.* **1981**, *20*, 3607.

(5) Anderson, G. K.; Lumetta, G. J. *Organometallics* **1985**, *4*, 1542.

(6) Han, I. M.; Elsevier, C. J.; Vrieze, K.; van Leeuwen, P. W. N. M. To be submitted for publication.

(7) Dekker, G. P. C. M.; Elsevier, C. J.; Vrieze, K.; van Leeuwen, P. W. N. M. *Organometallics* **1992**, *11*, 1598.

(8) de Graaf, W.; Boersma, J.; van Koten, G. *Organometallics* **1990**, *9*, 1479.

(9) Rülke, R. E.; Han, I. M.; Elsevier, C. J.; Vrieze, K.; van Leeuwen, P. W. N. M.; Roobeek, C. F.; Zoutberg, M. C.; Wang, Y. F.; Stam, C. H. *Inorg. Chim. Acta* **1990**, *169*, 5. Rülke, R. E.; Elsevier, C. J.; Vrieze, K.; van Leeuwen, P. W. N. M. To be submitted for publication.

(10) Koga, N.; Morokuma, K. *J. Am. Chem. Soc.* **1985**, *107*, 7230. Koga, N.; Morokuma, K. *J. Am. Chem. Soc.* **1986**, *108*, 6136. Sakaki, S.; Kitaura, K.; Morokuma, K.; Ohkubo, K. *J. Am. Chem. Soc.* **1983**, *105*, 2280.

(11) Durfee, L. D.; Rothwell, I. P. *Chem. Rev.* **1988**, *88*, 1059.

(12) Carmona, E.; Contreras, L.; Poveda, M. L.; Sanchez, L. J. *J. Am. Chem. Soc.* **1991**, *113*, 4322 and references cited therein.

Table II. ^{1}H and ^{31}P{^{1}H} NMR Data for Compounds 1–12

	^{1}H[a]		^{31}P[a]
compd	δ(M–CH_3)[b]	δ(N(CH_3)$_2$)[b]	δ(P)[b]
1		2.24	0.5
2		3.42 [35]	6.2 [3882]
3a		3.23 {1.6}	31.8
3b[c]		2.16	12.3
3b[c,d]		2.75 (d)/1.36 (d) {12}	14.9/9.7
4a	0.54 [75] {3.1}	3.14 [12]	19.8 [4821]
4b	0.57 [66] {1.5}	3.03 [11]	14.8 [5596]
4c	0.32 [71] {2.5}	3.15 [10]	17.5 [4837]
4d	0.34 [62] {1.5}	3.03 [10]	13.8 [4539]
4e	0.31 [71] {3.1}	3.16 [12]	16.9 [4836]
5a	0.65 {3.2}	2.94	39.6
5b	0.64 {0.9}	2.83	44.5
5c	0.44 {2.2}	2.78	44.5
5d	0.38 {0.8}	2.85	42.2
5e	0.38 {2.2}	2.87	41.9
6a*[g]	0.72 [57] {4.7}	2.15	22.9 [4760]
6a	1.73 [11]	2.95 [10]	8.8 [5065]
6b–e*[g]	0.57 [74] {5.6}	3.54 [17]	26.4 [3560]
6b[e]	1.89 [16]	3.40 [n.o.]	14.2 [3968]
6e[f]	1.73	3.17	6.2
7a	1.83	2.75	20.1 (9)
7b	1.93	2.71	23.9 (9)
7c	1.93 {1.6}	2.69	27.5
7d	1.88	2.75	23.5
7e	1.84	2.72	22.8
8		2.18	−15.4
9	0.36 [70] {4.2}	2.79 [12]	9.2 [4765]
10a	0.45 {3.5}	2.61	29.5
10b	0.43	2.48	37.0
11*[g]	0.68 [56] {4.6}	2.16	13.3 [3972]
11	1.69 [9.5]	2.59 [10]	1.6 [5052]
12a	1.83 {1.4}	2.45	14.7
12b	1.91	2.47	12.3

[a] In $CDCl_3$ unless otherwise stated. [b] *J*(Pt–H) or *J*(Pt–P) values are given in brackets; *J*(P–H) values are given in braces; *J*(C–P) values are given in parentheses. [c] In CD_2Cl_2. [d] 213 K. [e] Under 25 bar of CO, low resolution of spectrum due to high-pressure tube. [f] Only a very small amount formed, and hence no coupling constants could be obtained. [g] Intermediate observed during carbonylation.

Recently we observed in our laboratory that insertion of CO in the Pd–CH_3 bond proceeded much faster for (bpy)Pd(CH_3)Cl (bpy = 2,2′-bipyridyl)[6] than for (P-P)-Pd(CH_3)Cl (P-P = diphosphine ligand).[7] Fast CO insertion was also found by de Graaf et al. for (tmeda) Pd(CH_3)Br (tmeda = *N,N,N′,N′*-tetramethylethanediamine).[8] Also very interestingly, rapid carbonylation was recently observed in the case of palladium-methyl complexes with terdentate nitrogen ligands, e.g. [(terpy)Pd(CH_3)]$^+$Cl$^-$.[9] The observation that the diphosphine complexes reacted slower than the diimine and diamine complexes prompted us to address the following problems: (i) the rate of CO insertion in complexes containing hemilabile phosphine–amine ligands as compared to that in complexes containing the diamine, diimine, and diphosphine ligands and (ii) the question whether the hemilabile ligand acts as a bi- or monodentate ligand in the course of the carbonylation. Therefore, we synthesized the Pd(II) and Pt(II) complexes (P–N)M(CH_3)Cl and [(P–N)M(CH_3)(L)]$^+$Y$^-$ (P–N = 1-(dimethylamino)-8-(diphenylphosphino)naphthalene (PAN), 1-(dimethylamino)-3-(diphenylphosphino)propane (PC_3N); Y$^-$ = BF_4^-, $SO_3CF_3^-$, L = CH_2Cl_2, CH_3CN) and studied the insertion of CO in the M–CH_3 bond.

Results and Discussion

In Table I the numbering of the compounds discussed in this paper has been given.

Synthesis and Characterization of 1-(Dimethylamino)-8-(diphenylphosphino)naphthalene (PAN; 1).

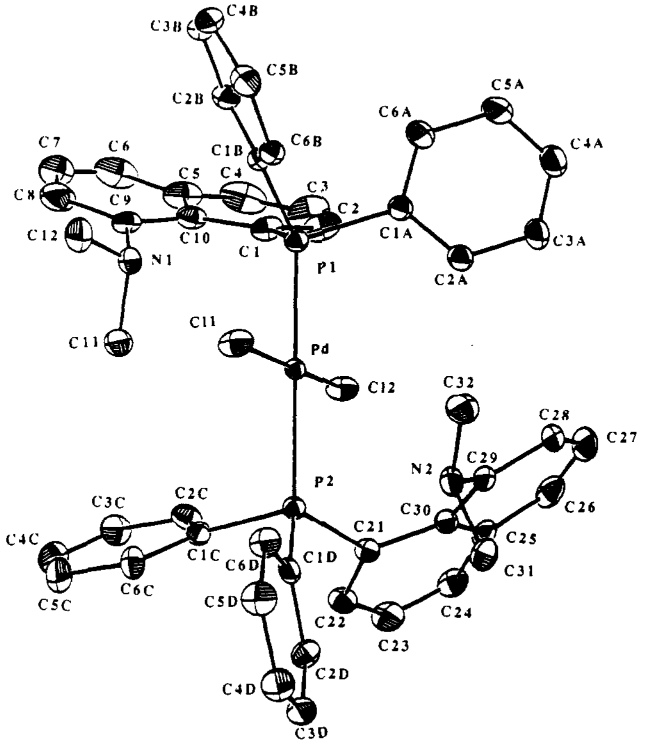

Figure 2. Ortep drawing of the molecular structure of (PAN)$_2$PdCl$_2$ (**3b**).

The ligand 1-(dimethylamino)-8-(diphenylphosphino)-naphthalene[13] (PAN; 1 in Figure 1) was prepared according to the method of Horner,[13] which was slightly modified (see Experimental Section). The ligand formed was purified by column chromatography over basic Al_2O_3 using benzene as the eluent. The ^{1}H NMR resonance of the dimethylamino group of the PAN ligand appears at 2.24 ppm in $CDCl_3$ (Table II), while the ^{31}P NMR spectrum shows a resonance at 0.5 ppm. The PAN ligand is slowly oxidized, even in the solid state, when exposed to air. The ligand 1-(dimethylamino)-3-(diphenylphosphino)propane (PC_3N; 8 in Figure 1) was prepared and purified according to published methods.[14]

Synthesis and Characterization of (PAN)$_x$MCl$_2$ (M = Pt, *x* = 1 (2); M = Pd, *x* = 1 (3a), 2 (3b)). The complexes (PAN)PtCl$_2$ (**2**) and (PAN)PdCl$_2$ (**3a**) were prepared to study the coordination behavior of **1**, which may act as a monodentate ligand via the phosphorus or the nitrogen atom or as a bidentate ligand via both the phosphorus and the nitrogen atoms. The complexes were prepared by reaction of (COD)MCl$_2$ (M = Pd, Pt) with 1 equiv of **1** (see Experimental Section). When (COD)PdCl$_2$ was made to react with 2 equiv of **1**, (PAN)$_2$PdCl$_2$ (**3b**) was formed. The same reaction for (COD)PtCl$_2$ resulted in the formation of **2** only. In the complexes **2** and **3a** the ligand coordinates via both the phosphorus and the nitrogen atoms, as could be inferred from the NMR spectra; the N(CH_3)$_2$ resonance is shifted to higher frequency, and in **2** a coupling constant ^3J(Pt–H) of 35 Hz on the N(CH_3)$_2$ resonance is observed. In **3b** the ligand coordinates only via the phosphorus atom, as the N(CH_3)$_2$ resonance moved only slightly as compared to that in **1**.

Single-Crystal X-ray Structure Determination of (PAN)$_2$PdCl$_2$ (3b) (Y.F.W., C.H.S.). The molecular structure consists of a distorted-square-planar *trans*-

---

[13] Horner, L.; Simons, G. *Phosphorus Sulfur Relat. Elem.* **1983**, *15*, 165.

[14] Anderson, G. K.; Kumar, R. *Inorg. Chem.* **1984**, *23*, 4064.

Table III. Selected Bond Distances (Å) and Angles (deg) for $(PAN)_2PdCl_2$ (3b)

Pd–P(1)	2.368 (2)	Pd–Cl(1)	2.298 (2)
Pd–P(2)	2.386 (2)	Pd–Cl(2)	2.299 (2)
P(1)–Pd–P(2)	171.00 (5)	P(2)–Pd–Cl(1)	87.46 (2)
P(1)–Pd–Cl(1)	83.99 (6)	P(2)–Pd–Cl(2)	93.92 (6)
P(1)–Pd–Cl(2)	94.48 (6)	Cl(1)–Pd–Cl(2)	176.70 (6)

$(PAN)_2PdCl_2$ molecule (Figure 2). The PAN ligands coordinate to the Pd center only via the phosphorus atom and are in mutual trans positions. The P–Pd–P angle of 171.00 (5)° and the Cl–Pd–Cl angle of 176.70 (6)° differ significantly from 180° (Table III). For *trans*-$PdCl_2(PPh_3)_2 \cdot {}^1/_2\text{-}p\text{-}C_6H_4Cl_2$,[15] *trans*-$PdCl_2\{(Me_2$-*neo*-Men)P$\}_2$,[16] and *trans*-$PdCl_2\{(Me_2Men)P\}_2]$,[16] smaller deviations were observed: the P–Pd–P angles were 175.23 (4), 173.3 (2), and 175.5 (5)°, respectively, while the Cl–Pd–Cl angles were 177.76 (5), 176.7 (2), and 180°, respectively.

The Cl–Pd–P angles of 83.99 (6), 87.46 (2), 94.48 (6), and 93.92 (6)° for $(PAN)_2PdCl_2$ all differ significantly more from 90° than the Cl–Pd–P angles in *trans*-$PdCl_2(PPh_3)_2 \cdot {}^1/_2\text{-}p\text{-}C_6H_4Cl_2$ (86.81 (4)–92.95 (5)°),[15] *trans*-$PdCl_2\{(Me_2$-*neo*-Men)P$\}_2$ (89.7 (2)–90.4 (2)°),[16] or *trans*-$PdCl_2\{(Me_2Men)P\}_2$ (87.8 (3)–92.3 (3)°).[16] The larger distortions from 180° for the P–Pd–P and Cl–Pd–Cl angles and from 90° for the Cl–Pd–P angles in $(PAN)_2PdCl_2$ relative to the distortions found for the reported complexes mentioned above[15,16] are ascribed to the bulkiness of the (dimethylamino)naphthyl group bonded to the phosphorus atoms in $(PAN)_2PdCl_2$. The Pd–Cl distances of 2.298 (2) and 2.299 (2) Å in $(PAN)_2PdCl_2$ lie in the range found for other Pd–Cl distances.[15,16] The Pd–P distances of 2.368 (2) and 2.386 (2) Å in $(PAN)_2PdCl_2$ are significantly longer than the Pd–P distances usually found for trans P–Pd–P complexes: 2.31–2.36 Å.[15-17] This elongation of the Pd–P bond is also ascribed to the bulkiness of the (dimethylamino)naphthyl group, as in other complexes containing bulky substituents at the phosphine atoms, i.e. [*trans*-$\{(tBu)_2P(CH_2)_2CH(CH_3)(CH_2)_2P(tBu)_2\}PdCl_2]_2$[18] and [*trans*-$\{(tBu)_2P(CH_2)_5P(tBu)_2\}PdCl_2]_2$,[19] the Pd–P distances range from 2.372 (6) to 2.388 (6) Å and from 2.370 (4) to 2.379 (4) Å, respectively.

Dynamic Behavior of 3b. At room temperature **3b** in CD_2Cl_2 partially (55%) dissociated into **3a** and **1**, as shown by the appearance of three single resonances for the dimethylamino groups in the ^1H NMR spectra as well as three single resonances in the $^{31}P\{^1H\}$ NMR spectra (300 MHz for ^1H). The ability of **1** to coordinate in a bidentate mode as well as in a monodentate mode is reflected by the formation of both **3a** and **3b**, respectively. When this solution was cooled to 220 K, the ^1H NMR signal due to the dimethylamino groups of **3b** split up into two $N(CH_3)_2$ resonances, and the ^{31}P signal at 12.3 ppm likewise split into two resonances at 9.7 and 14.9 ppm (Table II). The signals of **3a** and **1** did not show significant changes in the ^1H and $^{31}P\{^1H\}$ NMR spectra upon cooling to 220 K. These data indicate that above 220 K the two isomers present for **3b** are involved in an intramolecular exchange process. From the ^{31}P resonances a $\Delta G^{\ddagger}$ value of 45 kJ·mol^{-1} for this interconversion process was obtained.[20]

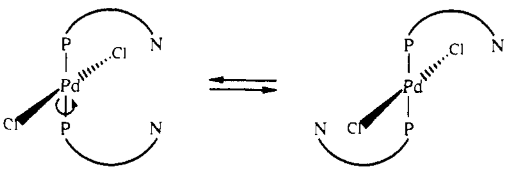

cis-N,N *trans*-N,N

Figure 3. The two conformers of **3b**: cis-N,N and trans-N,N.

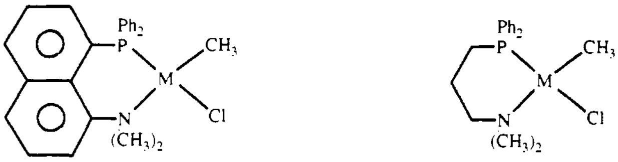

Figure 4. Schematic structure of $(PAN)M(CH_3)Cl$ (left; M = Pt (**4a**), Pd (**5a**)) and of $(PC_3N)M(CH_3)Cl$ (right; M = Pt (**9**), Pd (**10a**)).

Table IV. Selected Bond Distances (Å) and Angles (deg) for $(PAN)Pd(CH_3)Cl$ (5a)

Pd–P	2.2009 (8)	Pd–Cl	2.3869 (8)
Pd–N	2.276 (2)	Pd–C(13)	2.068 (2)
P–Pd–N	86.20 (6)	Cl–Pd–P	176.98 (3)
P–Pd–C(13)	90.07 (7)	Cl–Pd–N	96.50 (6)
N–Pd–C(13)	175.70 (9)		

Various mixtures of $CD_3C(O)CD_3$ with CD_2Cl_2 were used to study the effect of variations in the polarity of the solvent on the concentrations of the two isomers of **3b** at 220 K. With an increasing amount of $CD_3C(O)CD_3$, i.e. increasing polarity of the solvent, the relative intensity of the signal at 9.7 ppm increased with respect to the signal at 14.9 ppm, indicating that the former originates from the isomer with the higher dipole moment. The coalescence temperature was independent of the $CD_3C(O)CD_3/CD_2Cl_2$ ratio in the range of 0.0–1.0. From the above findings it may be concluded that the interconversion occurs between the more polar isomer cis-N,N (^{31}P signal at 9.7 ppm), in which both dimethylamino groups are in relative cis positions to each other, and the isomer trans-N,N (^{31}P signal at 14.9 ppm), with both dimethylamino groups trans to each other. The most likely mechanism for this intramolecular exchange process involves rotations about the Pd–P bonds (Figure 3).

Synthesis and Characterization of $(PAN)M(CH_3)Cl$ (M = Pt (4a), Pd (5a)). The complexes $(PAN)Pt(CH_3)Cl$ (**4a**) and $(PAN)Pd(CH_3)Cl$ (**5a**) were prepared by addition of **1** to $(COD)M(CH_3)Cl$ (M = Pd, Pt) in benzene at room temperature (see Experimental Section). It should be noted that $(PAN)_2M(CH_3)Cl$, which would be analogous to **3b**, could not be obtained. The ligand coordinates to the metal via both the phosphorus and the nitrogen atoms, as evidenced by the ^1H and $^{31}P\{^1H\}$ NMR spectra (Table II).[21,22] The ^1H NMR spectra show a high-frequency shift for the $N(CH_3)_2$ resonance from 2.24 ppm for free PAN to 3.14 ppm (^3J(Pt–H) = 12 Hz) in **4a** and 2.94 ppm in **5a**, respectively. The methyl resonances appear as doublets at 0.57 ppm (^3J(P–H) = 3.1 Hz) (**4a**) and 0.64 ppm (^3J(P–H) = 3.2 Hz) (**5a**). The magnitudes of these coupling constants show a cis relationship[22,23] between the two

---

[15] Kitano, Y.; Kinoshita, Y.; Nakamura, R.; Ashida, T. *Acta Crystallogr.* **1983**, *C39*, 1015.

[16] Kan, K.; Miki, K.; Kai, Y.; Yasuoka, N.; Kasai, N. *Bull. Chem. Soc. Jpn.* **1978**, *51*, 733.

[17] Maitlis, P. M. In *The Organic Chemistry of Palladium*; Maitlis, P. M., Stone, F. G. A., West, R., Eds.; Academic Press: New York, 1972; Vol. I, and references therein.

[18] Al-Salem, N. A.; McDonald, W. S.; Markham, R.; Norton, M. C.; Shaw, B. L. *J. Chem. Soc., Dalton Trans.* **1980**, 59.

[19] McDonald, W. S. *Acta Crystallogr.* **1979**, *B35*, 3051.

[20] $\Delta G^{\ddagger}$ was calculated by using the equation $\Delta G^{\ddagger} = (19 \times 10^{-3})T_C(9.97 + \log T_c - \log|\nu_A - \nu_B|)$, where T_c is the coalescence temperature (K) and $|\nu_A - \nu_B|$ the shift difference (Hz) of the two exchange sites in the limiting low-temperature spectra. See: Günther, H. *NMR Spectroscopy, An Introduction*; Wiley: New York, 1973; p 243.

[21] Rauchfuss, T. B.; Patino, F. T.; Roundhill, D. M. *Inorg. Chem.* **1975**, *14*, 652.

[22] de Graaf, W.; Harder, S.; Boersma, J.; van Koten, G.; Kanters, J. A. *J. Organomet. Chem.* **1988**, *358*, 545.

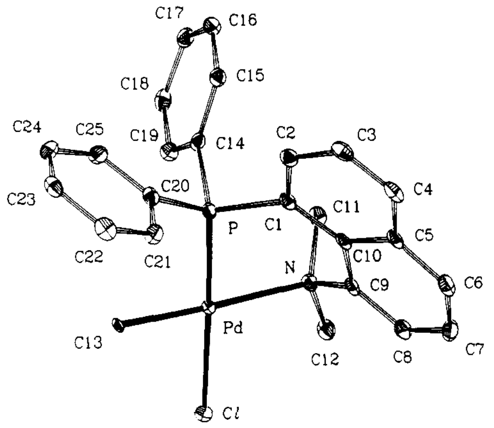

Figure 5. Thermal motion ellipsoid plot drawn at the 50% probability level for the molecular structure of (PAN)Pd(CH_3)Cl (**5a**) (H atoms are omitted for clarity).

groups which have a large trans influence,[24] i.e. the phosphorus atom and the methyl group. A coupling constant ^1J(Pt–P) of 4821 Hz for **4a** ($^{31}P\{^1H\}$ NMR) was measured, which is indicative of a ligand with a weak trans influence, in our case a chloride anion, bonded in a trans position relative to the phosphorus atom.[25] These data prove that in solution compounds **4a** and **5a** are present with the geometry as shown in Figure 4. A single-crystal X-ray analysis of **5a** is in agreement with this structure proposed on the basis of the NMR data.

Single-Crystal X-ray Structure Determination of (PAN)Pd(CH_3)Cl (5a) (W.J.J.S., A.L.S.). For (PAN)-Pd(CH_3)Cl (**5a**) (Figure 5) the Pd–P distance of 2.2009 (8) Å (Table IV) is comparable to the Pd–P distance of 2.207 (3) Å in (*o*-(diphenylphosphino)-*N*,*N*-dimethylbenzylamine)Pd(CH_3)Br[22] and is much shorter than the Pd–P distance of 2.241 (1) Å in (*N*,*N*-dimethyl-α-methyl-*o*-(butylphenylphosphino)benzylamine)PdCl_2.[26]

The Pd–N distance of 2.276 (2) Å (Table IV) is significantly longer than the Pd–N distances in (*o*-(diphenylphosphino)-*N*,*N*-dimethylbenzylamine)Pd(CH_3)Br[22] (2.220 (6) Å) and in (*N*,*N*,*N*′,*N*′-tetramethylethanediamine)Pd-$(CH_3)_2$[27] (2.200 (2) and 2.197 (2) Å). This long Pd–N distance is very likely due to the strong trans influence of the methyl group, while also the rigidity of the ligand might cause elongation of the Pd–N bond. The Pd–C(13) distance of 2.068 (2) Å (Table IV) is between the Pd–C distances of 2.142 (8) Å for (*o*-(diphenylphosphino)-*N*,*N*-dimethylbenzylamine)Pd(CH_3)Br[22] and both 2.026 (3) and 2.029 (3) Å for (tmeda)Pd$(CH_3)_2$.[27] The Pd–Cl distance of 2.3869 (8) Å (Table IV) is not significantly different from the Pd–Cl distance of 2.386 (1) Å in (*N*,*N*-dimethyl-α-methyl-*o*-(butylphenylphosphino)benzylamine)PdCl_2.[26]

Synthesis and Characterization of Ionic [(PAN)M(CH_3)]$^+$Y$^-$ and [(PAN)M(CH_3)(L)]$^+$Y$^-$ Complexes (M = Pt (4b–e), Pd (5b–e)). The ionic complexes [(PAN)M-(CH_3)]$^+$Y$^-$ and [(PAN)M(CH_3)(L)]$^+$Y$^-$ (M = Pt: Y$^-$ = $SO_3CF_3^-$ (**4b**); Y$^-$ = BF_4^- (**4c**); M = Pt, L = CH_3CN, Y$^-$ = $SO_3CF_3^-$ (**4d**); Y$^-$ = BF_4^- (**4e**); M = Pd: Y$^-$ = $SO_3CF_3^-$ (**5b**); Y$^-$ = BF_4^- (**5c**); M = Pd, L = CH_3CN, Y$^-$ = $SO_3CF_3^-$ (**5d**); Y$^-$ = BF_4^- (**5e**)) were prepared by addition of $AgBF_4$ or $AgSO_3CF_3$ to a solution of the chloride complex (PAN)M-(CH_3)Cl (M = Pt (**4a**), Pd (**5a**)) in CH_2Cl_2 in the presence or absence of 1 equiv of CH_3CN (see Experimental Section). The ^1H and $^{31}P\{^1H\}$ NMR spectra (Table II) show little difference between the ionic complexes (**4b–e** and **5b–e**) and the chloride compounds (**4a** and **5a**). For **4b–e** the coupling constants ^1J(Pt–P) are in the range of 4800–5600 Hz, which means that very weakly coordinating groups, e.g. BF_4^-, $SO_3CF_3^-$, CH_3CN, or CH_2Cl_2, are in trans positions to the phosphorus atom. Therefore, the coordination of the P–N ligands in the ionic complexes is assumed to be the same as in the chloride complexes, i.e. the methyl group cis to the phosphorus atom.

Scheme II. Proposed Mechanism for the Insertion of CO in the Pt–CH_3 Bond of the Complexes (P–N)Pt(CH_3)Cl (P–N = PAN (4a), PC_3N (9))[a]

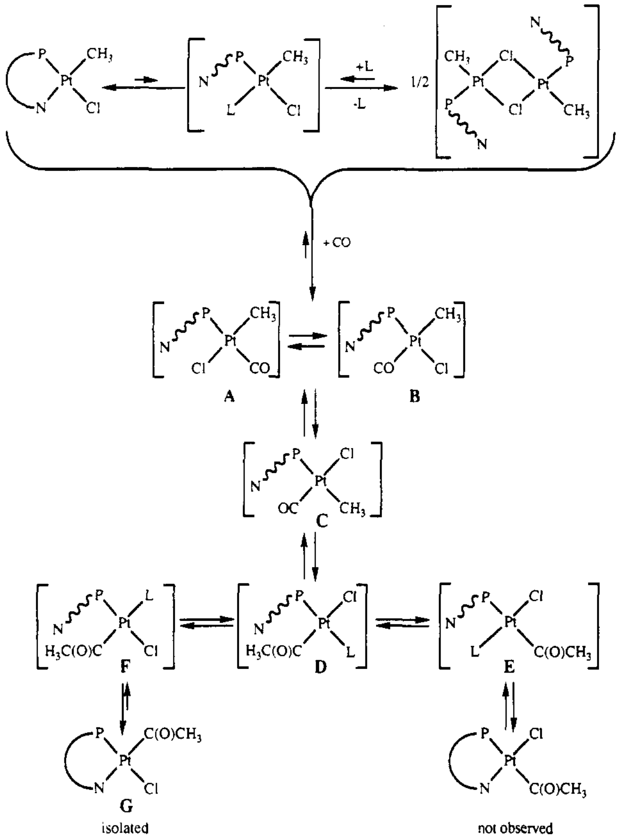

[a] L = CH_2Cl_2. Intermediate B is observed as **6a*** and **11***. The acyl product G is observed as **6a** and **11**.

Synthesis and Characterization of (PC_3N)Pt-(CH_3)Cl (9a), (PC_3N)Pd(CH_3)Cl (10a), and [(PC_3N)-Pd(CH_3)(CH_3CN)]$^+$$SO_3CF_3^-$ (10b). Complexes (PC_3-N)Pt(CH_3)Cl (**9**), (PC_3N)Pd(CH_3)Cl (**10a**), and [(PC_3N)-Pd(CH_3)(CH_3CN)]$^+$$SO_3CF_3^-$ (**10b**), containing the flexible P-N ligand PC_3N (**8**)[14] (Figure 1), were prepared in a way similar to that for **4a**, **5a**, and **5d** (see Experimental Section). Comparison of the complexes **9**, **10a**, and **10b** with the complexes **4a**, **5a**, and **5d** (Table II) shows that the latter have the same coordination geometry as depicted in Figure 4.

Reaction of the PAN-Pt Complexes 4a–e and the PC_3N-Pt Complex 9 with CO. The reaction of (P-N)-Pt(CH_3)Cl (P-N = PAN (**4a**), PC_3N (**9**)) with CO has been followed with time as a function of the temperature by both NMR and IR spectroscopy. In the ^1H and $^{31}P\{^1H\}$ NMR spectra clear evidence has been obtained, in the case of both PAN and PC_3N, for the existence of an interme-

---

[23] Appleton, T. G.; Bennett, M. A.; Tomkins, I. B. *J. Chem. Soc., Dalton Trans.* **1976**, 439.

[24] Hartley, F. R. *Chem. Soc. Rev.* **1973**, *2*, 163. Appleton, T. G.; Clark, H. C.; Manzer, L. E. *Coord. Chem. Rev.* **1973**, *10*, 335. Babkov, A. V. *Polyhedron* **1988**, *7*, 1203.

[25] Scrivanti, A.; Botteghi, C.; Toniolo, L.; Berton, A. *J. Organomet. Chem.* **1988**, *344*, 261.

[26] Takenaka, A.; Sasada, Y.; Yamamoto, K.; Tsuji, J. *Bull. Chem. Soc. Jpn.* **1977**, *50*, 3177.

[27] de Graaf, W.; Boersma, J.; Grove, D.; Spek, A. L.; van Koten, G. *Recl. Trav. Chim. Pays-Bas* **1988**, *107*, 299.

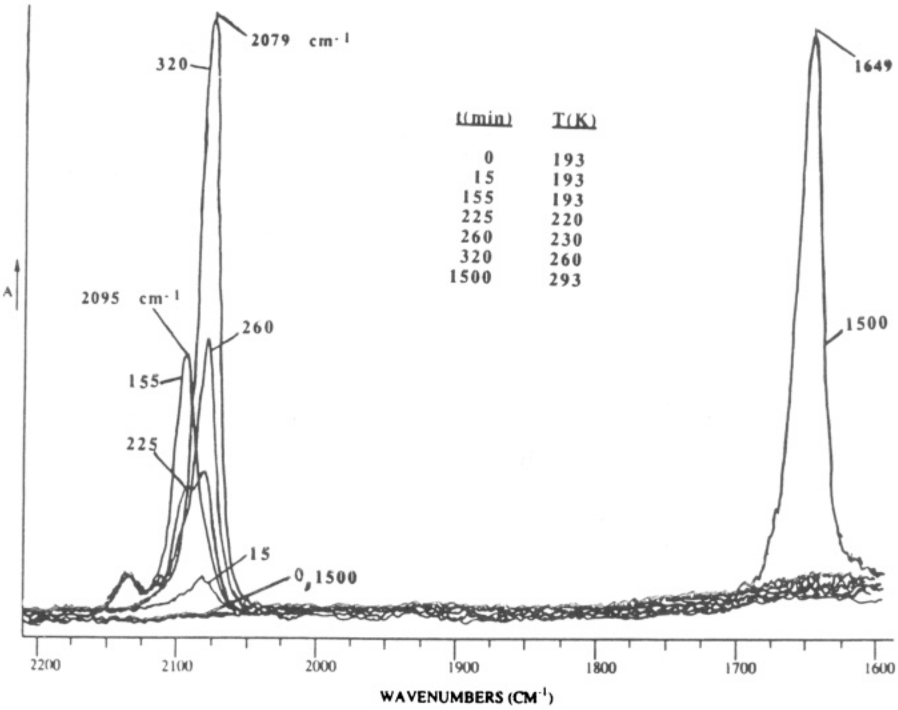

Figure 6. Change of the IR CO absorption spectrum during the reaction of (PAN)Pt(CH_3)Cl (**4a**) with CO as a function of time and temperature (*A* = absorbance).

diate with configuration B (Scheme II).

Above 250 K the N(CH_3)$_2$ signal at 3.14 ppm of (PAN)Pt(CH_3)Cl (**4a**) was converted to a signal at 2.15 ppm *without* a coupling ^3J(Pt–H), showing the presence of an intermediate, **6a*** (B in Scheme II, Table II), with a dissociated dimethylamino group. The CH_3–Pt resonance at 0.54 ppm changed into a signal at 0.72 ppm, with an increase of ^3J(P–H) from 3.4 to 4.4 Hz while the coupling ^2J(Pt–H) decreased from 75 to 57 Hz, the latter being indicative of a ligand with a stronger trans influence than the nitrogen atom, e.g. CO, coordinated opposite to the methyl group. The ^{31}P{^{1}H} NMR spectrum has a signal at 22.9 ppm with a coupling constant ^1J(Pt–P) of 4760 Hz indicative of a chloride anion trans to the phosphorus atom (Table II).

Similar to the PAN case, one intermediate, **11** (B in Scheme II, Table II), could be observed for the reaction of (PC_3N)Pt(CH_3)Cl (**9**) with CO between 250 K and room temperature, i.e. a species with a CH_3–Pt signal at 0.68 ppm (^2J(Pt–H) = 56 Hz and ^3J(P–H) = 4.6 Hz) and a N(CH_3)$_2$ resonance at 2.20 ppm *without* a coupling ^3J(Pt–H). The ^{31}P{^{1}H} NMR signal was observed at 13.3 ppm (^1J(Pt–P) = 3972 Hz). These values are very similar to that of the PAN intermediate B (**6a***, Table II) in the carbonylation of **4a** to **6a**.

At room temperature these intermediates B convert quantitatively to the final Pt–acyl products **6a** and **11** (G in Scheme II), as a CH_3C(O)–Pt signal appeared at 1.73 ppm (^3J(Pt–H) = 11 Hz) and a N(CH_3)$_2$ resonance at 2.95 ppm (^3J(Pt–H) = 10 Hz) for P-N = PAN. In the case of PC_3N these values are 1.69 ppm (^3J(Pt–H) = 9.5 Hz) and 2.59 ppm (^3J(Pt–H) = 10 Hz), respectively. The presence of Pt coupling on the N(CH_3)$_2$ signals reveals that in G (Scheme II) the dimethylamino group is coordinated again to the Pt atom. The ^{31}P{^{1}H} NMR signals were observed at 8.8 ppm (^1J(Pt–P) = 5065 Hz) for P-N = PAN and at 1.6 ppm (^1J(Pt–P) = 5052 Hz) for P-N = PC_3N. The high coupling values indicate that a chloride anion rather than the acyl group is trans to the phosphorus atom, since an acyl group trans to P would give a much lower coupling, on the order of 1750–1850 Hz.[28]

It is of interest to note that the configuration of the thermodynamically stable acyl products **6a** and **11** (G in Scheme II) is analogous to that of the starting compounds, i.e. the nitrogen atom trans to the carbon atom and the phosphorus atom trans to a chloride anion.

IR studies, which can give information about short-lived intermediates not observable by NMR spectroscopy, as a function of temperature and time of the reaction of CO with (PAN)Pt(CH_3)Cl (**4a**) showed at 193 K the formation of two CO stretching bands at 2135 cm^{-1} and a broad band located at 2095 cm^{-1} with a shoulder at approximately 2079 cm^{-1} (Figure 6). The absorption at 2135 cm^{-1} is due to free CO dissolved in CD_2Cl_2, as checked with a blank experiment at 193 K. The absorption at 2095 cm^{-1} has been assigned tentatively to intermediate [cis P, trans CH_3 (Pt–CO)], i.e. **6a*** (B in Scheme II, as observed by NMR), which was based on the IR spectrum of the analogous intermediate B of Scheme I, which has a CO band at 2106 cm^{-1}.[29] The shoulder at 2079 cm^{-1} is assigned to intermediate C (Scheme II) with the configuration [cis P, cis CH_3 (Pt–CO)], since the band is close to the frequency of 2087 cm^{-1} reported to belong to [cis P, cis Ph (Pt–CO)],[29] intermediate C in Scheme I. The bands at 2095 and 2079 cm^{-1} are each about 10 cm^{-1} lower than those of the analogous aryl intermediates B and C in Scheme I. Heating this solution to 220 K resulted in the increase of the CO band at 2079 cm^{-1} with the simultaneous decrease of intensity of the 2095-cm^{-1} absorption, while the band at 2135 cm^{-1} had fully disappeared. In intermediate C (Scheme II) the CO and methyl groups are cis to each other, while the methyl group is trans to the phosphorus atom, a situation very conducive for CO insertion. Indeed, warming of the solution to room temperature resulted in the growth of a band at 1649 cm^{-1} at the expense of the 2079-cm^{-1} band (Figure 6). An analogous situation has

---

[28] Albinati, A.; von Gunten, U.; Pregosin, P. S.; Rüegg, H. *J. Organomet. Chem.* **1985**, *295*, 239. van Leeuwen, P. W. N. M.; Roobeek, C. F.; Frijns, J. H. G.; Orpen, A. G. *Organometallics* **1990**, *9*, 1211.

[29] Anderson, G. K.; Cross, R. J. *J. Chem. Soc., Dalton Trans.* **1979**, 1246.

Scheme III. Possible Routes for the Carbonylation of the Complexes (P-N)Pd(CH$_3$)Cl and (P-N)M(CH$_3$)(L)Y (M = Pd(II), Pt(II); Y$^-$ = SO$_3$CF$_3^-$, BF$_4^-$; L = CH$_3$CN, CH$_2$Cl$_2$; P-N = PAN, PC$_3$N)[a]

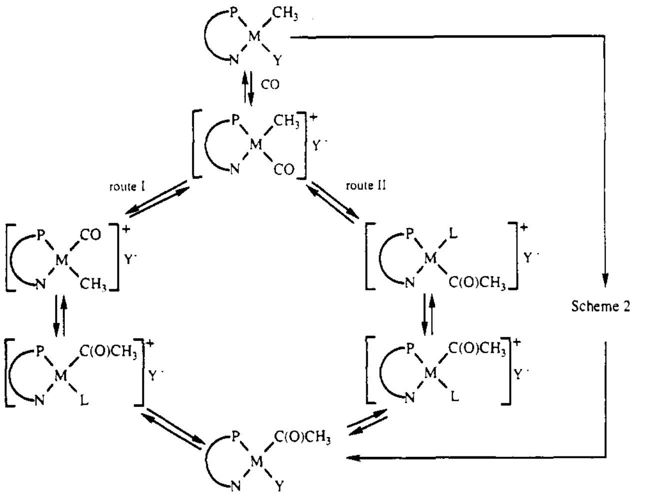

[a] For L = CH$_2$Cl$_2$, Y$^-$ might replace L at the metal center.

been observed for the conversion of intermediate C to the Pt-aroyl complex of Scheme I,[29] for which a CO band has been reported at 1620 cm^{-1} (*trans*-(PPh$_3$)$_2$Pt(C(O)Ph)Cl).[30] It should be noted that we have assumed that the PAN ligand has become monodentate bonded, also in C, via the phosphorus atom, a type of coordination which the PAN can easily adopt and which we confirmed by NMR spectroscopy for intermediate B (**6a***).

Very similar observations have been made for the carbonylation of (PC$_3$N)Pt(CH$_3$)Cl (**9**), which could be converted to (PC$_3$N)Pt(C(O)CH$_3$)Cl (**11**) (Table II, G in Scheme II). The IR spectrum at 193 K shows low-intensity signals at 2133, 2105, and 2075 cm^{-1}, which may be assigned to free CO and intermediates A [trans P, cis CH$_3$ (Pt–CO)] and C [cis P, cis CH$_3$ (Pt–CO)] in Scheme II, with CO frequencies very similar in magnitude to the PAN case. At 223 K the band at 2133 cm^{-1} had fully disappeared, while two bands of low intensity were observed at about 2097 and 2079 cm^{-1}. The latter is assigned to C in Scheme II, the small shift (4 cm^{-1}) of the band as compared with the 2075-cm^{-1} absorption at 193 K being probably due to temperature effects. The band at about 2097 cm^{-1} is broad, which is likely the result of overlap of the band due to A at 2105 cm^{-1} (193 K) and 2092 cm^{-1} (293 K, see later). Subsequently at 293 K one observes only a band at 2092 cm^{-1}, which is assigned to intermediate B, [cis P, trans CH$_3$ (Pt–CO)] (**11***) in Scheme II in analogy with intermediate B (**6a***), 2095 cm^{-1}), found for PAN, and a shoulder at 2079 cm^{-1}, which means that in addition to intermediate B also intermediate C (Scheme II) is present at 293 K. In the final IR spectrum at 293 K after a longer reaction time one observes the conversion of the bands at 2092 and 2079 cm^{-1} to a band at 1649 cm^{-1}, which is characteristic for the acyl product **11** (i.e. G in Scheme II).

Considering the total picture of the carbonylation of (P-N)Pt(CH$_3$)Cl, the spectroscopic data for both PAN and PC$_3$N clearly indicate that there is a buildup of species B, i.e. **6a*** and **11*** (Scheme II), which is apparently quite stable, as it is observed by NMR and also IR spectroscopy. It should be noted that for the PC$_3$N complex intermediate B is formed at higher temperatures than for the PAN complex, which we cannot explain thus far. Intermediate A, which is only observable by IR spectroscopy for P-N = PC$_3$N and then only at very low temperatures, has clearly a short lifetime, as it was not observed by NMR methods. Intermediate C, which was not observed by NMR spectroscopy, also has a short lifetime but could be observed quite clearly by IR methods for P-N = PAN and PC$_3$N. It should be noted that intermediate C is observed rather early, which might be due to the relative high temperature of CO when it is introduced at the start of the experiment. On the basis of the combined IR and NMR data it seems very likely that the carbonylation proceeds as shown in Scheme II. The unsaturated intermediates D–F (Scheme II) could not be observed, but D and F must be present in order to arrive at the thermodynamically stable acyl product G, i.e. **6a** and **11** (Scheme II). Scheme II bears of course a strong resemblance to Scheme I,[2] the difference being that in Scheme II intermediate C may be formed from both A and B. Furthermore, we have observed the intermediates prior to insertion, i.e. A–C, and the final acyl product G in one reaction sequence in the case of P-N = PC$_3$N by means of IR spectroscopy. Finally, it should be noted that for these hemilabile ligands the easily dissociable dimethylamino group plays in an intramolecular pathway the role of the dissociated PPh$_3$ ligand in Scheme I.

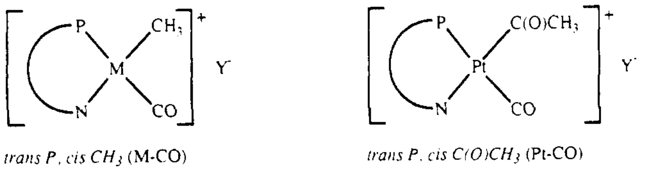

Figure 7. Observed intermediates **6b–e*** and **7b–e*** in the carbonylation of the M–CH$_3$ bond of complexes [(PAN)M(CH$_3$)(L)]$^+$Y$^-$ (M = Pt(II), Pd(II); **4b–e**, **5b–e**). The intermediate [trans P, cis CH$_3$ (M–CO)] (M = Pt(II), Pd(II) is formed prior to insertion, and the intermediate [trans P, cis C(O)CH$_3$ (Pt–CO)] is formed after insertion.

Carbonylation of the ionic Pt complexes **4b–e**, where Y$^-$ (SO$_3$CF$_3^-$, BF$_4^-$) is a good leaving group (**4b,c**) or not coordinating when CH$_3$CN is bonded to Pt (**4d,e**), all yielded only one type of intermediate, **6b–e***, which showed the presence of a terminal CO group in the IR spectrum at 2110 cm^{-1}. In the ^{1}H NMR spectrum the N(*CH*$_3$)$_2$ resonance appears at 3.53–3.55 ppm (^3J(Pt–H) = 16–18 Hz), which proves bonding of the nitrogen atom to the Pt atom (Table II). For the carbonylation of complexes **4d,e** the signal of the coordinated CH$_3$CN ligand (2.60 ppm) has disappeared while free CH$_3$CN was observed at 2.03 ppm. The ^{31}P{^{1}H} NMR signals of all ionic intermediates prior to insertion, **6b–e***, resonate at 26–27 ppm with a coupling constant ^1J(Pt–P) ranging from 3550 to 3580 Hz, indicating that the phosphorus atom is trans to CO,[29,31] which is in accord with the CO stretch of about 2110 cm^{-1}. We assign these data to intermediate [trans P, cis CH$_3$ (Pt–CO)], as depicted in Figure 7. This configuration, which we also see for the starting product and for the final product, is clearly a stable one.

This intermediate is shown in Scheme III as the first carbonylation intermediate leading to routes I and II. The formation of the acyl compound [(PAN)Pt(C(O)CH$_3$)]$^+$-

---

[30] Dent, S. P.; Eaborn, C.; Pidcock, A.; Ratcliff, B. *J. Organomet. Chem.* **1972**, *46*, C68.

[31] Anderson, G. K.; Cross, R. J. *J. Chem. Soc., Dalton Trans.* **1980**, 1434. Appleton, T. G.; Bennett, M. A. *Inorg. Chem.* **1978**, *17*, 738.

$SO_3CF_3^-$ (**6b**) in the reaction of **4b** with CO occurred only under CO pressure. The CH_3C(O)–Pt signal of the product **6b** appeared at 1.89 ppm with a coupling constant ^3J(Pt–H) of 16 Hz, while the N(CH_3)$_2$ signal was found at 3.40 ppm. The $^{31}P\{^1H\}$ NMR signal occurred at 14.2 ppm (^1J(Pt–P) = 3968 Hz), which value is clearly due to a CO group trans to the phosphorus atom. The acyl complex **6b**, the proposed geometry of which is shown in Figure 7, i.e. [trans P, cis C(O)CH_3 (Pt–CO)], decarbonylated upon releasing the CO pressure. Clearly a ligand, in this case CO, coordinated cis to the acyl group is needed to stabilize the Pt–acyl product. In view of the data it is reasonable to assume that the carbonylation of ionic complexes proceeds via either route I or route II (Scheme III). For both routes the P-N ligand remains chelate bonded.

Reaction of the PAN-Pd Complexes 5a–e and the PC_3N-Pd Complexes 10a,b with CO. The carbonylation of Pd compounds **5a–e** afforded a rather simple picture, since the chloride complex **5a** yielded directly the acyl product as evidenced by the values of the ^1H NMR signals of the CH_3C(O)–Pd and N(CH_3)$_2$ groups of the product **7a** (Table II), indicating that the P-N ligand is chelate bonded. The $^{31}P\{^1H\}$ NMR signal appeared for the acyl product **7a** at 20.9 ppm with a coupling constant ^2J(P–C) of 9 Hz when ^{13}CO was employed. This value is indicative of the acyl group being cis to the phosphorus atom. A trans orientation would have given a ^2J(P–C) value in the range 100–160 Hz.[29,32] The CO stretch was observed at 1693 cm^{-1}.

Also for the reactions of the compounds **5b–e** (Y^- = $SO_3CF_3^-$, BF_4^-; L = CH_3CN, CH_2Cl_2) acyl products **7b–e** were obtained with very similar NMR data and an IR signal at 1725 cm^{-1}. However, IR data also provided evidence for an intermediate with a CO signal around 2135 cm^{-1}, both at 193 and at 293 K. This frequency is identical with that of free CO, but at 293 K no free CO could be detected, as was checked with a blank experiment. This high frequency indicates that the CO group must be loosely bonded to the Pd atom in these ionic intermediates, which should then contain a chelate-bonded P-N ligand, i.e. [trans P, cis CH_3 (Pd–CO)] (Figure 7).

The reactions of the ionic Pd complexes depend strongly on the coordinating power of the solvent, since for example in the reaction of **5c** with CO in CH_3CN instead of CH_2Cl_2 neither CO coordination nor CO insertion was observed.

Finally, both the neutral PC_3N complex **10a** and the ionic **10b** only yielded the acyl products **12a,b** (Table II), while no intermediates could be detected by either NMR or IR spectroscopy. Taking into consideration the above data, we tentatively assume that the carbonylation of the Pd(II) complexes proceeds via route I and/or II (Scheme III), although a route similar to that in Scheme II cannot be excluded rigorously.

Reaction Rates. Reaction rates in terms of half-life times $t_{1/2}$ were measured in CD_2Cl_2 at 25 bar of CO by means of NMR measurements in a high-pressure tube.[33] The rates for the Pt complexes measured at 293 K are given in Table V, while the rates for the Pd complexes obtained at 258 K are presented in Table VI. In Tables V and VI also some literature data are given for relevant bpy and dppp complexes for comparison.[6,7]

Table V. Carbonylation of (P-N)Pt(CH_3)Cl and Comparison with (L-L)Pt(CH_3)Cl[a]

compd	T, K	$t_{1/2}$[b]
(PAN)Pt(CH_3)Cl (**4a**)	293	10 ± 3 min
(PC_3N)Pt(CH_3)Cl (**9**)	293	55 ± 5 min
(dppp)Pt(CH_3)Cl	293	1 week
(dppe)Pt(CH_3)Cl	293	no reacn

[a] In CD_2Cl_2, 25 bar of CO, high-pressure NMR tube.[33] [b] Time after which half of the Pt–CH_3 complex is converted into the Pt–C(O)CH_3 complex.

Table VI. Carbonylation of (P-N)Pd(CH_3)Cl and [(P-N)Pd(CH_3)(CH_3CN)$^+SO_3CF_3^-$ and Comparison with (L-L)Pd(CH_3)Cl and [(L-L)Pd(CH_3)(CH_3CN)]$^+SO_3CF_3^-$[a]

compd	T, K	$t_{1/2}$, min[b]	ref
(PAN)Pd(CH_3)Cl (**5a**)	258	35 ± 4	*c*
(PC_3N)Pd(CH_3)Cl (**10a**)	258	120 ± 6	*c*
(bpy)Pd(CH_3)Cl	235	<1.5 ± 0.5	6
(dppp)Pd(CH_3)Cl	235	26 ± 3	7
(dppe)Pd(CH_3)Cl	305	170 ± 5	7
[(PAN)Pd(CH_3)(CH_3CN)]$^+SO_3CF_3^-$ (**5d**)	258	105 ± 5	*c*
[(PC_3N)Pd(CH_3)(CH_3CN)]$^+SO_3CF_3^-$ (**10b**)	258	33 ± 4	*c*
[(bpy)Pd(CH_3)(CH_3CN)]$^+SO_3CF_3^-$	235	<1.5 ± 0.5	6
[(dppp)Pd(CH_3)(CH_3CN)]$^+SO_3CF_3^-$	235	<1.5 ± 0.5	7
[(dppe)Pd(CH_3)(CH_3CN)]$^+SO_3CF_3^-$	235	2.5 ± 0.5	7

[a] In CD_2Cl_2, 25 bar of CO, high-pressure NMR tube.[33] [b] Time after which half of the Pd–CH_3 complex is converted into the Pd–C(O)CH_3 complex. [c] This work.

Figure 8. Influence of P-P and N-N ligands on the relative charge density on the R group and the carbon atom of the CO molecule (Y^- = Cl^-, BF_4^-, $SO_3CF_3^-$). For simplicity's sake Y^- is pictured outside the coordination shell, but Y^- might also be in the first coordination sphere on a fifth position.

When we consider first the rate of reaction of the complexes with the bidentate ligand L-L, it is interesting to note (Table VI) that in the case of the palladium chloride complexes (L-L)Pd(CH_3)Cl the rates decrease in the order bpy > dppp > PAN > PC_3N > dppe.[6,7] A similar sequence was observed for the ionic palladium complexes [(L-L)-Pd(CH_3)(L)]$^+Y^-$ (Table VI). However, for these compounds the order of the P-N ligands was reversed, i.e. PC_3N > PAN. In the consideration of these trends it is useful to remember that for most reactions involving palladium compounds we observed only one intermediate ([trans P, cis CH_3 (Pd–CO)], in Figure 7) with the P-N ligand bidentate bonded, the methyl and CO groups being cis to each other and Y^-, including Cl^-, being (partly) dissociated. If we assume that the migratory insertion takes place via the four-coordinate intermediates of route I or II (Scheme III), which is reasonable in view of theoretical studies,[1,10] we may compare the rates with the rates of the bpy and dppp complexes (Table VI).

Previously, we have found[6,9] that the Pd(II) complexes containing bidentate N-N ligands and even terdentate ligands react much faster than those with P-P ligands. These findings can be rationalized by using simple arguments involving the charge density on the methyl group and on the carbon atom of the CO group (Figure 8).

In the case of the symmetric bidentate ligands it is argued that although the methyl group trans to the phosphorus atom is more nucleophilic than the methyl group trans to the nitrogen atom due to the higher trans influence of the former,[24] the N-N complexes react much faster, since the CO group trans to the nitrogen atom is more electro-

---

(32) Bennett, M. A.; Rokicki, A. *J. Organomet. Chem.* **1983**, *244*, C31. Brown, J. M.; Cooley, N. A. *Organometallics* **1990**, *9*, 353.

(33) Roe, D. C. *J. Magn. Reson.* **1985**, *63*, 388.

philic than that trans to the phosphorus atom.[34] Apparently, for migratory insertion the electrophilic character of the carbon atom of the CO group is more important than the nucleophilic character of the carbon atom of the methyl group.

When we now consider the influence of the bidentate-bonded P-N ligand, we would naively suspect the magnitude of the rates to be within those of the N-N and P-P complexes. However, when we look more closely at the actual structure of the initial complex for routes I and II, i.e. [trans P, cis CH_3 (M–CO)], the situation is unfavorable for insertion, since the methyl group is trans to the nitrogen atom and CO trans to the phosphorus atom. When formation of the observed acyl product proceeds via route I, the first step is isomerization of the initial starting complex [trans P, cis CH_3 (M–CO)] to form the energetically unfavorable [cis P, trans CH_3 (M–CO)], which is activated toward migratory insertion, as the methyl group is trans to P and CO trans to N. Migratory insertion leads directly to the thermodynamically stable acyl product, i.e. with the carbon atom trans to N and cis to P. Route II starts with migratory insertion from the thermodynamically stable complex [trans P, cis CH_3 (M–CO)] to form the kinetic acyl product where the methyl group is trans to P and cis to N. Isomerization has to take place to form the thermodynamically favorable product which was mentioned for route I.

The initial and final products have the same configuration, i.e. the carbon atom cis to the phosphorus atom. Thus, the reaction via route I or II has to pass via either an extra barrier of a prerearrangement reaction (route I) or a large kinetic barrier in the migration step (route II) to the final acyl product. This is not the case for the N-N and P-P complexes, where no isomerization has to take place. On these grounds it can be understood that the order is N-N > P-P > P-N.

It is rather surprising that, in the case of the palladium chloride complexes, the PAN complex reacted faster than the PC_3N complex, while the opposite was found for complexes with good leaving anionic groups such as $SO_3CF_3^-$ and BF_4^-. The order PC_3N > PAN would be as expected, since also in the case of the diphosphines the complex of the more flexible dppp ligand reacts faster than the complex of the rigid dppe ligand;[7] as suggested by theoretical calculations,[10] the angle subtended at the metal by the two P atoms increases much more for dppp than for dppe when one goes from the initial state to the transition state. The order PAN > PC_3N for the chloride complexes, both for Pd and Pt (Tables V and VI), is therefore not very well understandable, unless these chloride complexes react via the path in Scheme II. The PAN complex is more strained than the PC_3N complex, and hence the PAN ligand might adopt a monodentate coordination more easily than the PC_3N ligand. Isomerization of the monodentate-coordinated species is assumed to occur readily. It should be noted that during the carbonylation of the palladium chloride complexes no intermediates could be observed by either NMR or IR spectroscopy.

From Table VI it may also be deduced that the palladium complexes with good leaving anionic groups react much faster than the chloride complexes. In this instance one may see clearly that the rates are greatly enhanced by making the metal easily accessible for CO. In the case of the ionic Pd(II) complexes in CD_2Cl_2 the CH_3CN ligand easily makes place for CO but coordinates with sufficient strength to stabilize the acyl intermediates in routes I and II of Scheme III. The order PC_3N > PAN for the ionic complexes is understandable, since PC_3N will allow isomerizations of the bidentate coordinated complexes more readily because of its higher flexibility as compared to that of PAN.

Furthermore, it may be observed from Tables V and VI that the platinum chloride complexes react much more slowly than the analogous palladium complexes, which is as expected, since Pt(II) complexes are in general kinetically much more stable. At first sight it is surprising that for the platinum complexes the dppp complex reacted more slowly than the P-N compounds (Table V). However, it has been shown that these Pt(P-N) complexes react via the path in Scheme II, while the dppp ligand very likely remains chelate-bonded, (also proposed by Anderson et al.[5]), as certainly in the case of Pt the Pt-P bonds are very strong indeed, while the chloride anion does not easily dissociate. Thus, it is much more difficult for (dppp)Pt(CH_3)Cl to offer an accessible coordination site than for the analogous PAN and PC_3N compounds.

Finally, we wish to mention that no information could be gleaned from the experiments about the migratory insertion step or about the necessary isomerizations preceding this step in route I or following this step in route II of Scheme III.

Experimental Section

All reactions and manipulations were carried out under purified nitrogen using Schlenk techniques. ^{1}H and ^{31}P{^{1}H} NMR spectra were recorded on a Bruker AC 100 spectrometer at 100.13 and 40.53 MHz, respectively, and a Varian VXR 300 spectrometer at 299.94 and 121.42 MHz, respectively. Shifts are relative to $(CH_3)_4Si$ (^{1}H) and 85% H_3PO_4 (^{31}P) as external standards, where positive shifts are to high frequency. IR spectra were recorded on a Nicolet 7199 B FT-IR spectrometer. CH_2Cl_2 was dried over P_2O_5. Benzene, diethyl ether, pentane, and THF were dried over Na wire. All solvents were distilled from the respective desiccants and stored under nitrogen. (COD)$PtCl_2$ (COD = 1,5-cyclooctadiene),[35] (COD)$PdCl_2$,[36] (COD)Pd(CH_3)Cl,[9,37] 1-(dimethylamino)-8-lithionaphthalene,[38] and 1-(dimethylamino)-3-(diphenylphosphino)propane (PC_3N; 8[14]) were prepared according to published methods. $Sn(CH_3)_4$ was obtained from Merck. Silver trifluoromethanesulfonate ($AgSO_3CF_3$) and silver tetrafluoroborate ($AgBF_4$) were obtained from Janssen Chimica. Ultra High Purity CO gas (NMR experiments) and CP-grade CO gas (synthetic experiments) were obtained from Matheson.

(COD)Pt(CH_3)Cl. To a solution of (COD)$PtCl_2$ (2.46 g, 6.6 mmol) in a 1:1 mixture of CH_2Cl_2/methanol (100 mL) was added 1 equiv of $Sn(CH_3)_4$ (1.18 g, 0.91 mL, 6.6 mmol). After reaction for 24 h the resulting colorless solution was filtered over Celite on a G-4 filter and evaporated to dryness. The white product was washed with several 10-mL portions of diethyl ether. The product was recrystallized from a mixture of CH_2Cl_2/diethyl ether. The yield was 1.84 g (79%) of pale yellow crystals.

1-(Dimethylamino)-8-(diphenylphosphino)naphthalene (PAN; 1). To a cooled (−30 °C) solution of 1-(dimethylamino)-8-lithionaphthalene (2.72 g, 15.4 mmol) in THF (60 mL) was added 1 equiv of Ph_2PCl (3.39 g, 15.4 mmol), followed by slowly warming the solution to room temperature. After it was stirred for 2 days, the yellow solution was evaporated to dryness.

---

(34) Cotton, F. A. *Inorg. Chem.* **1964**, *3*, 702. Horrocks, W. D., Jr.; Taylor, R. C. *Inorg. Chem.* **1963**, *2*, 723.

(35) Clark, H. C.; Manzer, L. E. *J. Organomet. Chem.* **1973**, *59*, 411.

(36) Chatt, J.; Vallarino, L. M.; Venanzi, L. M. *J. Chem. Soc.* **1957**, 3413.

(37) van Leeuwen, P. W. N. M.; Roobeek, C. F. Eur. Pat. Appl. 380162, 1990.

(38) Jastrzebski, J. T. B. H.; van Koten, G.; Goubitz, K.; Arlen, C.; Pfeffer, M. *J. Organomet. Chem.* **1983**, *246*, C75.

Subsequently the crude product was dissolved in benzene and purified by filtration over a column of Al_2O_3. Evaporation of the resulting yellow solution afforded the pure product, a yellow powder, in 2.83 g (52%) yield. Anal. Calcd for $C_{24}H_{22}NP$: C, 81.10; H, 6.24; P, 8.71. Found: C, 80.48; H, 6.18; P, 8.64.

(PAN)PtCl$_2$ (2). To a solution of (COD)PtCl$_2$ (0.31 g, 0.83 mmol) in 15 mL of CH_2Cl_2/benzene (1:1) was added a solution of PAN (0.35 g, 0.98 mmol) in 5 mL of benzene. After the mixture was stirred for 2 h, the reaction was complete and an orange precipitate had formed. The product was collected by filtration, washed with benzene (3 × 5 mL) and pentane (3 × 5 mL), and recrystallized from CH_2Cl_2/pentane. The yield was 0.43 g (84%) of orange powder. Anal. Calcd for $C_{24}H_{22}NPCl_2Pt$: C, 46.39; H, 3.57; P, 4.98. Found: C, 46.20; H, 3.44; P, 4.85.

(PAN)PdCl$_2$ (3a). This compound was prepared using the same method as for **2**, except that (COD)PdCl$_2$ was used instead of (COD)PtCl$_2$: yield 79% of yellow powder. Anal. Calcd for $C_{24}H_{22}NPCl_2Pd$: C, 54.11; H, 4.17; P, 5.81. Found: C, 54.01; H, 4.24; P, 5.78.

(PAN)$_2$PdCl$_2$ (3b). This compound was prepared using the same method as for **3a**, except that 2 equiv of PAN was added instead of 1 equiv. The yield amounted to 80% of orange powder. Anal. Calcd for $C_{48.5}H_{45}N_2P_2Cl_3Pd$: C, 62.60; H, 4.90; P, 6.66. Found: C, 62.23; H, 4.86; P, 6.57.

(PAN)Pt(CH$_3$)Cl (4a). To a solution of (COD)Pt(CH$_3$)Cl (0.29 g, 0.82 mmol) in benzene/CH_2Cl_2 (1:1) (15 mL) was added a solution of 1 equiv of PAN (0.30 g, 0.84 mmol) in benzene (10 mL). After the mixture was stirred for 2 h, the white product was filtered off and washed with benzene (3 × 5 mL) and pentane (3 × 5 mL). The product was recrystallized from a mixture of CH_2Cl_2/diethyl ether. The yield was 0.32 g (65%) of white powder. Anal. Calcd for $C_{25}H_{25}NPClPt$: C, 49.96; H, 4.19; P, 5.15. Found: C, 49.83; H, 3.87; P, 4.97.

(PAN)Pt(CH$_3$)(SO$_3$CF$_3$) (4b). To a rapidly stirred solution of **4a** (0.18 g, 0.30 mmol) in 15 mL of CH_2Cl_2 was added 1 equiv $AgSO_3CF_3$ (0.08 g, 0.30 mmol). The immediately formed white suspension was filtered into 20 mL of cooled (−20 °C) diethyl ether while it was rapidly stirred. The white powder that deposited in the diethyl ether was filtered off, washed with diethyl ether (2 × 3 mL) and pentane (2 × 3 mL), and dried under vacuum. The yield was 0.14 g (65%) of white powder. Anal. Calcd for $C_{26}H_{25}NPO_3SF_3Pt$: C, 43.70; H, 3.53; P, 4.33. Found: C, 43.91; H, 3.74; P, 4.18.

(PAN)Pt(CH$_3$)(BF$_4$) (4c). The same procedure was used as for **4b** except that $AgBF_4$ was used instead of $AgSO_3CF_3$: yield 58% of pale brown powder. Anal. Calcd for $C_{25}H_{25}NPBF_4Pt$: C, 46.03; H, 3.87; P, 4.75. Found: C, 46.12; H, 3.97; P, 4.67.

(PAN)Pt(CH$_3$)(CH$_3$CN)(SO$_3$CF$_3$) (4d). To a rapidly stirred solution of **4a** (0.21 g, 0.35 mmol) in 15 mL of CH_2Cl_2/CH_3CN (14:1) was added dropwise a solution of $AgSO_3CF_3$ (0.09 g, 0.35 mmol) in 2 mL of CH_3CN. The immediately formed white suspension was filtered into 30 mL of cooled (−20 °C) diethyl ether while it was rapidly stirred. The resulting white powder was filtered off, washed with diethyl ether (3 × 5 mL) and pentane (2 × 5 mL), and dried under vacuum. The yield was 0.19 g (72%) of white powder. Anal. Calcd for $C_{28}H_{28}N_2PO_3SF_3Pt$: C, 44.50; H, 3.74; P, 4.10. Found: C, 44.22; H, 3.83; P, 4.09.

(PAN)Pt(CH$_3$)(CH$_3$CN)(BF$_4$) (4e). The same procedure was used as for **4d**, except that $AgBF_4$ was used instead of $AgSO_3CF_3$: yield 64% of pale brown powder. Anal. Calcd for $C_{27}H_{28}N_2PBF_4Pt$: C, 46.77; H, 4.07; P, 4.47. Found: C, 46.77; H, 4.17; P, 4.69.

(PAN)Pd(CH$_3$)Cl (5a), (PAN)Pd(CH$_3$)(SO$_3$CF$_3$) (5b), (PAN)Pd(CH$_3$)(BF$_4$) (5c), (PAN)Pd(CH$_3$)(CH$_3$CN)(SO$_3$CF$_3$) (5d), and (PAN)Pd(CH$_3$)(CH$_3$CN)(BF$_4$) (5e). The same procedures were used as for the preparation of **4a–e** except that (COD)Pd(CH$_3$)Cl was used instead of (COD)Pt(CH$_3$)Cl: yield 82% of off-white powder (**5a**), 68% of white powder (**5b**), 60% of pale brown powder (**5c**), 72% of white powder (**5d**), 63% of white powder (**5e**). Anal. Calcd for $C_{25}H_{25}NPClPd$ (**5a**): C, 58.61; H, 4.92; P, 6.05. Found: C, 58.76; H, 4.95; P, 5.88. Anal. Calcd for $C_{26}H_{25}NPO_3SF_3Pd$ (**5b**): C, 49.89; H, 4.03; P, 4.95. Found: C, 49.85; H, 3.78; P, 4.92. Anal. Calcd for $C_{25}H_{25}NPBF_4Pd$ (**5c**): C, 53.27; H, 4.47; P, 5.49. Found: C, 53.11; H, 4.28; P, 5.35. Calcd for $C_{28}H_{28}N_2PO_3SF_3Pd$ (**5d**): C, 50.42; H, 4.23; P, 4.64. Found: C, 50.48; H, 4.35; P, 4.61. Anal. Calcd for $C_{27}H_{28}N_2PBF_4Pd$ (**5e**): C, 53.63; H, 4.67; P, 5.12. Found: C, 53.42; H, 4.81; P, 5.08.

Table VII. Crystallographic Data for Compounds 3b and 5a

	3b	**5a**
	(a) Crystal Data	
formula	$C_{48}H_{44}N_2P_2PdCl_2 \cdot 0.5CH_2Cl_2$	$C_{25}H_{25}NPPdCl$
mol wt	930.66	512.33
cryst syst	triclinic	monoclinic
space group	$P\bar{1}$ (No. 2)	$P2_1/n$ (No. 14)
a, Å	12.837 (2)	11.418 (1)
b, Å	17.518 (3)	15.088 (1)
c, Å	10.788 (3)	12.434 (1)
α, deg	91.07 (2)	
β, deg	112.87 (2)	99.81 (1)
γ, deg	100.27 (2)	
V, Å^3	2189.1 (6)	2110.7 (3)
Z	2	4
D_{calc}, g cm^{-3}	1.43 (3)	1.6121 (2)
$F(000)$	946	1040
μ, cm^{-1}	63.8	10.8
cryst size, mm	0.08 × 0.08 × 0.13	0.50 × 0.15 × 0.10
	(b) Data Collection	
temp, K	293	100
θ_{min}, θ_{max}	2.5, 55	1.35, 26.48
radiation	Cu Kα, 1.5418 Å	Mo Kα (Zr-filtered), 0.710 73 Å
scan type	$\omega/2\theta$	$\omega/2\theta$
$\Delta\omega$, deg		$0.60 + 0.35 \tan \theta$
horiz and vert aperture, mm	4.4, 4	3.0, 5.0
ref reflns	−3,0,2, 020	−2,0,−2, 1,−3,0, 0,−2,−2
data set	h, −13 to +13; k −18 to +18; l, 0 to 11	h, −13 to 13; k, −18 to 0; l, 0 to 14
total no. of data	5469	4538
total of unique data	5469	4168
no. of obsd data	4334 ($I > 2.5\sigma(I)$)	3551 ($I > 2.5\sigma(I)$)
	(c) Refinement	
no. of refined params	506	272
weighting scheme	$w = 1/(6.94 + F_{obs} + 0.015F_{obs}^2)$	$w = 1.0/\sigma^2(F)$
final R, R_w, S	0.044, 0.065	0.025, 0.026, 1.49
$(\Delta/\sigma)_{av}$ in final cycle	0.08	0.028
min, max residual density, e/Å^3	−0.6, 0.6	−0.56, 0.42

(PC$_3$N)Pt(CH$_3$)Cl (9). The same procedure was used as for the preparation of **4a**: yield 68% of white powder. Anal. Calcd for $C_{18}H_{25}NPClPt$: C, 41.82; H, 4.88; P, 5.99. Found: C, 41.96; H, 4.95; P, 5.89.

(PC$_3$N)Pd(CH$_3$)Cl (10a). To a solution of (COD)Pd(CH$_3$)Cl (0.19 g, 0.72 mmol) in 15 mL of benzene was added a solution of PC$_3$N (0.19 g, 0.72 mmol) in 10 mL of benzene. After the mixture was stirred for 1 h, the red-brown solution was filtered off and evaporated to dryness and the residue washed with benzene (2 × 5 mL) and pentane (2 × 5 mL). The product was recrystallized from a mixture of CH_2Cl_2/diethyl ether. The yield was 0.18 g (59%) of red-brown powder. Anal. Calcd for $C_{18}H_{25}NPClPd$: C, 50.49; H, 5.88; P, 7.23. Found: C, 50.48; H, 5.98; P, 6.93.

(PC$_3$N)Pd(CH$_3$)(CH$_3$CN)(SO$_3$CF$_3$) (10b). The same procedure was used as for the preparation of **4d**. Anal. Calcd for $C_{19}H_{25}NPO_3SF_3Pd$: C, 42.11; H, 4.65; P, 5.72. Found: C, 41.87; H, 4.79; P, 5.54.

Carbonylation of 4a,b, 5a,b, 9, and 10a,b (NMR High-Pressure Experiments). The complexes were dissolved in CD_2Cl_2 (0.15 mmol in 1.5 mL) and were, under a nitrogen atmosphere, transferred into the high-pressure NMR tube.[33] The NMR tube was cooled to 200 K, and subsequently a pressure of 25 bar of CO was applied. The tube was shaken five times and transferred to the NMR spectrometer. After 3 min the first spectrum could be obtained. During the reaction the tube was shaken after 30 and after 60 min.

Table VIII. Fractional Coordinates of the Non-Hydrogen Atoms and Equivalent Isotropic Thermal Parameters for 3b

	x	y	z	U_{eq},[a] Å^2
Pd	0.47794 (3)	0.21488 (2)	0.16842 (4)	0.0307 (2)
Cl1	0.37992 (13)	0.28765 (9)	0.00390 (17)	0.0538 (10)
Cl2	0.58259 (14)	0.14865 (11)	0.34022 (17)	0.0597 (10)
Cl3	−0.0638 (9)	0.4886 (8)	−0.1231 (10)	0.406 (13)
P1	0.63797 (13)	0.27149 (9)	0.11992 (15)	0.0410 (8)
P2	0.30315 (12)	0.17409 (8)	0.20008 (14)	0.0369 (8)
C1	0.6511 (6)	0.3746 (4)	0.0904 (7)	0.057 (4)
C2	0.6023 (7)	0.3912 (5)	−0.0416 (9)	0.080 (5)
C3	0.6142 (9)	0.4664 (5)	−0.0821 (12)	0.110 (8)
C4	0.6788 (10)	0.5257 (5)	0.0123 (12)	0.111 (8)
C5	0.7349 (8)	0.5151 (4)	0.1532 (12)	0.098 (7)
C6	0.8091 (10)	0.5751 (5)	0.2493 (14)	0.123 (9)
C7	0.8607 (8)	0.5631 (5)	0.3805 (11)	0.106 (7)
C8	0.8337 (8)	0.4907 (6)	0.4274 (12)	0.107 (7)
C9	0.7564 (6)	0.4286 (4)	0.3338 (9)	0.068 (5)
C10	0.7119 (6)	0.4373 (4)	0.1951 (8)	0.061 (4)
C11	0.6071 (7)	0.3626 (5)	0.3970 (9)	0.081 (5)
C12	0.7954 (7)	0.3280 (6)	0.4981 (8)	0.090 (6)
C21	0.1753 (5)	0.1782 (3)	0.0474 (6)	0.040 (3)
C22	0.1001 (5)	0.2244 (4)	0.0497 (7)	0.056 (4)
C23	0.0211 (6)	0.2461 (5)	−0.0674 (8)	0.069 (5)
C24	0.0204 (6)	0.2262 (5)	−0.1867 (7)	0.065 (4)
C25	0.0926 (6)	0.1761 (4)	−0.1992 (6)	0.059 (4)
C26	0.1002 (6)	0.1586 (5)	−0.3247 (7)	0.072 (5)
C27	0.1651 (7)	0.1069 (5)	−0.3356 (7)	0.077 (5)
C28	0.2247 (6)	0.0695 (4)	−0.2205 (7)	0.059 (4)
C29	0.2218 (5)	0.0863 (4)	−0.0969 (6)	0.048 (4)
C30	0.1635 (5)	0.1454 (4)	−0.0818 (6)	0.045 (3)
C31	0.3720 (6)	0.0151 (4)	0.0311 (8)	0.068 (5)
C32	0.1785 (6)	−0.0217 (4)	0.0158 (7)	0.059 (4)
N1	0.7151 (5)	0.3572 (3)	0.3786 (6)	0.062 (4)
N2	0.2684 (4)	0.0443 (3)	0.0157 (5)	0.048 (3)
C1a	0.6149 (5)	0.2258 (4)	−0.0473 (6)	0.051 (4)
C2a	0.5122 (5)	0.1784 (4)	−0.1288 (6)	0.052 (4)
C3a	0.4937 (6)	0.1450 (5)	−0.2552 (7)	0.068 (5)
C4a	0.5803 (7)	0.1597 (6)	−0.2998 (8)	0.086 (6)
C5a	0.6852 (7)	0.2045 (7)	−0.2218 (9)	0.107 (7)
C6a	0.7019 (7)	0.2371 (7)	−0.0935 (8)	0.102 (7)
C1b	0.7846 (5)	0.2564 (3)	0.2134 (6)	0.041 (3)
C2b	0.8821 (5)	0.3139 (4)	0.2313 (7)	0.054 (4)
C3b	0.9926 (5)	0.2988 (4)	0.2949 (7)	0.061 (4)
C4b	1.0068 (5)	0.2261 (5)	0.3362 (7)	0.065 (5)
C5b	0.9127 (6)	0.1691 (4)	0.3138 (7)	0.062 (4)
C6b	0.8002 (5)	0.1825 (4)	0.2525 (6)	0.047 (4)
C1c	0.3127 (5)	0.2546 (3)	0.3190 (6)	0.044 (3)
C2c	0.3122 (6)	0.3308 (4)	0.2806 (8)	0.064 (5)
C3c	0.3306 (7)	0.3927 (4)	0.3773 (9)	0.074 (5)
C4c	0.3496 (7)	0.3800 (4)	0.5072 (9)	0.080 (5)
C5c	0.3517 (7)	0.3050 (5)	0.5478 (8)	0.079 (5)
C6c	0.3326 (6)	0.2439 (4)	0.4530 (7)	0.059 (4)
C1d	0.2621 (5)	0.0904 (3)	0.2825 (5)	0.040 (3)
C2d	0.1481 (5)	0.0691 (3)	0.2672 (6)	0.049 (4)
C3d	0.1119 (6)	0.0076 (4)	0.3281 (7)	0.058 (4)
C4d	0.1910 (7)	−0.0329 (4)	0.4081 (7)	0.063 (4)
C5d	0.3037 (6)	−0.0122 (4)	0.4264 (7)	0.063 (4)
C6d	0.3402 (5)	0.0492 (4)	0.3639 (7)	0.054 (4)

[a] U_{eq} = one-third of the trace of the orthogonalized **U**.

Carbonylation of 4a,b, 5a,b, 9, and 10 (IR Low-Temperature Experiments). The complexes were dissolved in CH_2Cl_2 and were, under a nitrogen atmosphere, transferred into the low-temperature IR cell.[39] The IR cell was cooled to 190 K. After CO was bubbled through the solution for 2 min, IR spectra were recorded. IR spectra were measured at intervals of 10 min upon remaining at one temperature. When the temperature was raised, a temperature equilibration time of 3 min was taken.

Table IX. Final Coordinates and Equivalent Isotropic Thermal Parameters of the Non-Hydrogen Atoms for 5a

atom	x	y	z	U(eq),[a] Å^2
Pd	0.60803 (2)	0.33299 (1)	0.72890 (2)	0.0094 (1)
Cl	0.40706 (6)	0.29570 (5)	0.73910 (6)	0.0150 (2)
P	0.78990 (6)	0.37112 (5)	0.71143 (6)	0.0106 (2)
N	0.67785 (19)	0.32639 (16)	0.91143 (18)	0.0126 (7)
C(1)	0.8436 (2)	0.45379 (18)	0.8163 (2)	0.0120 (8)
C(2)	0.9340 (2)	0.50899 (19)	0.7946 (2)	0.0149 (9)
C(3)	0.9732 (3)	0.58247 (19)	0.8589 (2)	0.0170 (9)
C(4)	0.9152 (2)	0.60403 (19)	0.9422 (2)	0.0165 (9)
C(5)	0.8200 (2)	0.55231 (18)	0.9673 (2)	0.0139 (9)
C(6)	0.7569 (3)	0.58195 (19)	1.0487 (2)	0.0181 (9)
C(7)	0.6663 (3)	0.5339 (2)	1.0762 (2)	0.0188 (9)
C(8)	0.6397 (3)	0.4506 (2)	1.0276 (2)	0.0164 (9)
C(9)	0.6985 (2)	0.41789 (18)	0.9490 (2)	0.0128 (8)
C(10)	0.7877 (2)	0.47165 (18)	0.9091 (2)	0.0121 (8)
C(11)	0.7892 (2)	0.27481 (18)	0.9456 (2)	0.0142 (9)
C(12)	0.5871 (3)	0.2798 (2)	0.9622 (2)	0.0168 (9)
C(13)	0.5540 (2)	0.34628 (18)	0.5623 (2)	0.0087 (8)
C(14)	0.8957 (2)	0.27934 (18)	0.7274 (2)	0.0124 (8)
C(15)	1.0185 (2)	0.29253 (19)	0.7561 (2)	0.0136 (9)
C(16)	1.0953 (3)	0.2216 (2)	0.7740 (2)	0.0166 (9)
C(17)	1.0515 (3)	0.1356 (2)	0.7630 (2)	0.0170 (9)
C(18)	0.9314 (3)	0.12092 (19)	0.7314 (2)	0.0166 (9)
C(19)	0.8534 (3)	0.19282 (19)	0.7138 (2)	0.0164 (9)
C(20)	0.8110 (2)	0.42364 (18)	0.5842 (2)	0.0129 (8)
C(21)	0.7592 (3)	0.50640 (19)	0.5555 (2)	0.0168 (9)
C(22)	0.7635 (3)	0.54276 (19)	0.4541 (2)	0.0186 (9)
C(23)	0.8182 (2)	0.4977 (2)	0.3796 (2)	0.0166 (9)
C(24)	0.8687 (3)	0.4150 (2)	0.4061 (2)	0.0182 (9)
C(25)	0.8649 (2)	0.3780 (2)	0.5088 (2)	0.0161 (9)

[a] U(eq) = one-third of the trace of the orthogonalized **U**.

Structure Determination and Refinement of (PAN)$_2$PdCl$_2$ (3b). The crystal data, X-ray data collection parameters, and refinement data for **3b** are listed in Table VII. The reflections were measured on an Enraf-Nonius CAD4 diffractometer using graphite-monochromated Cu Kα radiation. Those with an intensity below the 2.5$\sigma(I)$ level were treated as unobserved. The structure was solved by means of the heavy-atom method based on the Pd positions. After anisotropic block-diagonal least-squares refinement a difference Fourier synthesis indicated the positions of the H atoms and revealed the presence of a broad peak of height 3 e/Å^3, centered at x = 0.064, y = 0.509, z = 0.133 (about 1.4 Å from the center of symmetry at 0, $^1/_2$, 0). This peak is probably due to the presence of a half-molecule of CH_2Cl_2 per molecule of the Pd complex, CH_2Cl_2 having been used as a solvent. An additional Cl atom was therefore introduced at the indicated position. The H atoms were also introduced but not refined. Final atomic coordinates and equivalent isotropic thermal parameters are listed in Table VIII. An empirical absorption correction was applied (DIFABS).[40] The calculations were carried out with XRAY76.[41] The atomic scattering factors were taken from Cromer and Mann[42] and the dispersion correction factors from ref 43.

Structure Determination and Refinement of (PAN)Pd(CH$_3$)Cl (5a). A yellowish block-shaped crystal was mounted on top of a glass fiber and transferred to an Enraf-Nonius CAD4 diffractometer for data collection. Unit cell parameters were determined from a least-squares treatment of the SET4 setting angles of 25 reflections with 13.9 < θ < 19.5°. The unit cell parameters were checked for the presence of higher lattice symmetry.[44] Data were corrected for Lp and for a linear decay (1.3%) of the intensity control reflections during the 69 h of X-ray exposure time, but not for absorption. The structure was solved with standard Patterson methods (SHELXS86[45]); refinement on F was carried out by full-matrix least-squares techniques. H atoms were introduced on calculated positions (C–H = 0.98 Å) and included in the refinement riding on their carrier atoms. All non-H

---

(39) Schilder, P. G. M.; Luyten, H.; Stufkens, D. J.; Oskam, A. *Appl. Spectrosc.*, submitted for publication.

(40) Walker, N.; Stuart, D. *Acta Crystallogr.* **1983**, *A39*, 158.

(41) Stewart, J. M. The XRAY76 System, Tech. Rep. TR446; Computer Science Center, University of Maryland: College Park, MD, 1976.

(42) Cromer, D. T.; Mann, J. B. *Acta Crystallogr.* **1968**, *A24*, 321.

(43) *International Tables for X-ray Crystallography*; Kynoch Press: Birmingham, U.K., 1974; Vol. IV.

(44) Spek, A. L. *J. Appl. Crystallogr.* **1988**, *21*, 578.

atoms were refined with anisotropic thermal parameters and H atoms with one common isotropic thermal parameter ($U = 0.0158$ (16) Å^2). Weights were introduced in the final refinement cycles; convergence was reached at $R = 0.025$.

Crystal data and numerical details of the structure determination are given in Table VII. Final atomic coordinates and equivalent isotropic thermal parameters are listed in Table IX. Neutral atom scattering factors were taken from Cromer and Mann[42] and corrected for anomalous dispersion.[46] All calculations were performed with SHELX76[47] and the EUCLID package[48] (geometrical calculations and illustrations) on a MicroVAX cluster.

Acknowledgment. The Netherlands Foundation for Chemical Research (SON) and The Netherlands Organization for Scientific Research (NWO) are thanked for financial support (A.L.S., W.J.J.S.). Thanks are also due to A. J. M. Duisenberg for the X-ray data collection of (PAN)Pd(CH_3)Cl (**5a**) and D. Heidenrijk for the collection of the X-ray data for $(PAN)_2PdCl_2$ (**3b**). We thank H. Luyten, P. G. M. Schilder, J. M. Ernsting, and J. H. G. Frijns for their technical assistance. We are grateful to Shell Reseach BV for financial support.

Supplementary Material Available: Tables of H atom coordinates, anisotropic thermal parameters, and bond distances and angles for **3b** and **5a** (12 pages). Ordering information is given on any current masthead page.

OM9106560

---

[45] Sheldrick, G. M. SHELXS86: Program for Crystal Structure Determination; University of Göttingen: Göttingen, Federal Republic of Germany, 1986.

[46] Cromer, D. T.; Liberman, D. *J. Chem. Phys.* **1970**, *53*, 1891.

[47] Sheldrick, G. M. SHELX76: Crystal Structure Analysis Package; University of Cambridge: Cambridge, U.K., 1976.

[48] Spek, A. L. The EUCLID Package. In *Computational Crystallography*, Sayre D., Ed.; Clarendon Press: Oxford, England, 1982; p 528.

Organoboranes. 54. Exploration of the Reactions of (α-Haloallyl)lithium with Organoborane Derivatives. Simple and Convenient Procedure for the Synthesis of Three-Carbon Homologated Boronate Esters and Terminal Alkenes

Herbert C. Brown,* Milind V. Rangaishenvi,[1a] and Seetharaman Jayaraman[1b]

H. C. Brown and R. B. Wetherill Laboratories of Chemistry, Purdue University, 1393 Brown Building, West Lafayette, Indiana 47907

Received December 9, 1991

The synthetic utility of (α-haloallyl)lithium generated in situ for the facile transfer reaction of various organoborane derivatives, such as R_3B, R_2BOR', and $RB(OR')_2$, has been explored. This has led to the synthesis of α-vinylboronate esters, $RCH(CH{=}CH_2)B(OR')_2$, which are readily isomerized thermally to the corresponding allylboronate esters with the boron atom on the less substituted carbon atom, $RCH{=}CHCH_2B(OR')_2$. Catalytic hydrogenation of these allylboronate esters furnishes saturated boronate esters, $RCH_2CH_2CH_2B(OR')_2$, providing a three-carbon homologation of the original $R{-}B{<}$ moiety. Protonolysis in place of hydrogenation affords the corresponding terminal alkenes $RCH_2CH{=}CH_2$.

In view of their synthetic promise, the reactions of organoboranes with carbenoid reagents bearing a potential leaving group, such as $LiCCl_3$, $LiCH_2SMe$, $LiCHCl_2$, $LiCH_2Cl$, and LiCHCl(OMe), have been the focal point of several investigations in the recent past.[2] Such one-carbon homologations of organoboranes have led to the synthesis of pheromones, L-ribose, amino acids, and α-chiral compounds[3] in high enantiomeric purities. The remarkable difficulty encountered in the generation of such unstable carbenoids has been circumvented by the discovery of the practicality of in situ procedures.[4-6] As a part of our ongoing program on the synthetic utility of the homologation of organoboranes, we became interested in developing a protocol for three-carbon homologation. This involves the generation of α-heteroatom-substituted allylic carbanions. A search of the literature revealed very few reports on the formation of α-substituted allylic carbanions and their regioselective reaction with electrophiles.[7] Suzuki et al. had utilized this methodology in the synthesis

---

[1] (a) Postdoctoral research associate on Grant CHE-8706102 from the National Science Foundation. (b) Postdoctoral research associate (on leave from India) on Grant CHE-8706102 from the National Science Foundation.

[2] (a) Matteson, D. S. *Chem. Rev.* **1989**, *89*, 1535 and references cited therein. (b) Brown, H. C. In *Comprehensive Organometallic Chemistry*; Wilkinson, G., Stone, F. G. A., Abel, E. W., Eds.; Pergamon Press: New York, 1983; Vol. 7, Chapter 45.1.

[3] Rangaishenvi, M. V.; Singaram, B.; Brown, H. C. *J. Org. Chem.* **1991**, *56*, 3286.

[4] (a) Matteson, D. S.; Hurst, G. D. *Organometallics* **1986**, *5*, 1465. (b) Cainelli, G.; Ronchi, A. U.; Bertini, F.; Grasselli, P.; Zubiiana, G. *Tetrahedron* **1971**, *27*, 6109.

[5] Sadhu, K. M.; Matteson, D. S. *Organometallics* **1985**, *4*, 1687.

[6] Brown, H. C.; Singh, S. M.; Rangaishenvi, M. V. *J. Org. Chem.* **1986**, *51*, 3150.

[7] (a) Evans, D. A.; Andrews, G. C.; Buckwalter, B. *J. Am. Chem. Soc.* **1974**, *96*, 5560. (b) Still, W. C.; Macdonald, T. L. *J. Am. Chem. Soc.* **1974**, *96*, 5561. (c) Biellmann, J. F.; Ducep, J. B. *Org. React.* **1982**, *27*, 1. (d) For a recent reference, see: Julia, M.; Verpeaux, J.; Zahneisen, T. *Synlett* **1990**, 769.